

## Simulating The Spread of Membrane Potential Changes in Arteriolar Networks

Glenis J. Crane\*, Michael L. Hines† and Timothy O. Neild\*

\*Department of Human Physiology, School of Medicine, Flinders University, Adelaide, South Australia, Australia.

† Department of Computer Science and Neuroengineering and Neuroscience Center, Yale University, New Haven, CT 06520, U.S.A.

Author for correspondence:

Glenis J. Crane  
Department of Human Physiology, Flinders University,  
GPO Box 2100, Adelaide 5001, Australia.  
email [magjc@flinders.edu.au](mailto:magjc@flinders.edu.au)  
telephone +61 8 8204 5304  
fax +61 8 8204 5768

### ABSTRACT

**Objective:** Our aim was to simulate the spread of membrane potential changes in microvascular trees and make the simulation programs accessible to other researchers. We have applied our simulations to demonstrate the implications of electrical coupling between arteriolar smooth muscle and endothelium.

**Methods:** A two-layered cable-like model of an arteriole has been used, and the assumptions involved in the approach explicitly stated. Several common experimental situations which involve the passive spread of membrane potential changes in microvascular trees were simulated. The calculations were performed using NEURON, a well established computer simulation program which we have modified for use with vascular trees.

**Results:** Simulated results show that membrane potential changes would probably not spread as far in the endothelium as they would in the smooth muscle of arterioles. Where feed arteries are connected to larger distributing arteries, passive spread alone may not explain the physiologically observed spread of diameter changes.

**Conclusions:** Simulated results suggest that the morphology of an arteriole, in which the muscle layer is much thicker than the endothelium, favours electrical conduction along smooth muscle rather than the endothelium. However, it appears that passive electrical spread is insufficient to explain the apparent spread of membrane potential changes in experimental situations. Active responses involving voltage dependent conductances may be involved, and these can also be included in our simulation.

### Key words:

arteriole, smooth muscle, endothelium, gap junction, electrical coupling

## INTRODUCTION

In many arteriolar networks changes in diameter initiated by a stimulus to one region spread to other regions of the arteriolar tree. This process is thought to play a major role in the control of blood flow in tissues such as skeletal muscle and the brain, where metabolic factors act on the smallest arterioles but the effects must spread upstream to feed arteries before blood flow changes significantly (15). A similar mechanism may be coordinating diameter changes in renal afferent arterioles (3,26,28).

It has been proposed that diameter changes result from the spread of membrane potential changes in the smooth muscle and endothelial layers of the arterioles, and there is good experimental evidence in support of this broad concept (22,30,31). However, many questions still remain to be answered. It is still not clear whether the spread of membrane potential changes is entirely passive or whether there is some regenerative activity involving voltage-activated channels. There are also questions concerning the extent of electrical coupling between the endothelial and muscle layers (30,31). For example, how does the passive spread of membrane potential changes in an arteriolar network differ when the smooth muscle and endothelium are electrically coupled, as opposed to when they are not? Does the morphology of an arteriole favour electrical conduction along one cell layer compared to the other?

In order to answer these questions we need to be able to predict the way in which membrane potential changes will spread through the tissues in vascular networks, and compare theoretical predictions with experimental results. Most attempts to examine basic electrical properties and conduction in vascular smooth muscle have involved the use of "cable" equations commonly used to describe the properties of nerve axons (1,6,11,17,31). These models describe the passive spread of membrane potential changes along a vessel, assuming that no voltage-sensitive conductances are activated. This approach has been extended to deal with branching networks and to account for the fact that cross section of an arteriole resembles that of a hollow cylinder (22). The one-layered hollow cylinder model is useful when dealing with passive electrical conduction in a microvascular network, but cannot be used to relate cellular properties such as membrane resistance to the properties of the whole network when coupling between layers is present. Although it can predict the way in which the relative magnitude of membrane potential changes will vary in a branching tree, it cannot predict the actual size of the membrane potential changes expected for a particular current. This is a serious practical limitation, and led us to develop the model described below.

In the model we describe here real values can be entered for cellular parameters such as membrane resistance, and the magnitude as well as the spacial decay of potential changes can be predicted. It is also possible to go beyond simple passive electrical properties and include voltage-sensitive conductances in the model, although we have not pursued this aspect here. Here we give some examples of the use of the model to illustrate the properties of arteriolar networks, and as an aid to experimental design.

## MATERIALS AND METHODS

### **Adaptation of the NEURON program for use on vascular trees.**

The spread of membrane potential changes in branching structures has been investigated mostly in the context of the dendritic trees of neurons (18,14). Although the calculations are complex, simulation programmes for general use have been written which have enabled neuroscientists to gain considerable insight into the electrical responses in dendritic trees (9,10). We have started with one of these computer simulation packages, the NEURON

simulation environment, and modified it for use with microvascular trees. Changes were made to the standard NEURON program to enable us to calculate the simultaneous spread of membrane potential changes along smooth muscle and endothelial cell layers of the arteriole wall, and also vary the electrical coupling between the layers.

NEURON is the product of a collaboration between M.L. Hines (Department of Computer Science, Yale University) and J.W. Moore (Department of Neurobiology, Duke University) and is freely available for download from either: <http://www.neuron.yale.edu> (Yale) or <http://neuron.duke.edu> (Duke). Files which include the modified code required to use NEURON for vascular tree simulations may be obtained either by email or on floppy disc from the first author.

All computation was performed using NEURON version 4.1 on a standard PC-style computer with an Intel Pentium 133MHz processor and 32Mbytes of memory.

### **Assumptions underlying the calculations**

Both arteriolar networks and neurones can be modelled as branching trees of cable-like structures. The conduction pathways in the neuronal model are axons or dendrites which are equivalent to solid cables. Current flowing in the neuronal cytoplasm following membrane conductance changes flows either across the membrane or to through the cytoplasm to other regions of the cell. In the arteriole model, both the smooth muscle layer and endothelium consist of cells which may be electrically coupled. Within either layer, when cells are coupled the layer will have properties similar to those of nerve axons. The description of their electrical properties by the neuronal "cable" equations is valid if both circumferential and radial voltage gradients are negligible (11,16). Our basic model of a microvessel consists of two coupled cables, and is summarised in figure 1.

[Figure 1 near here]

However, the arterioles differ in one important respect from nerve axons; they are hollow whereas nerve axons are solid. This becomes significant when dealing with branched structures where the diameter of the vessels is not the same throughout the network, and requires a modification of some of the fundamental cable equations (23). The changes that we made to the NEURON programme have allowed for this difference. Briefly, the changes involve applying special diameter-dependent weightings to the membrane property values; the exact methodology can be seen in the modified NEURON source code files that can be obtained from the first author.

The assumptions that we have made are:

*That the smooth muscle layer is only 1 cell thick.* In principle, each cell layer of smooth muscle should be treated as an additional cable in the model. Here we have represented the smooth muscle as a single cable, and so our model refers only to vessels with one layer of smooth muscle. Such vessels would be arterioles by most definitions, for example Rhodin (20) refers to arterioles as having a muscle layer "1 or 2" cells thick. The smooth muscle layer may have cells overlapping in some regions only, making thickness of the layer impossible to define in terms of number of cells, but a single layer seems valid for arterioles up to 90 $\mu$ m in diameter (29).

*That there are no circumferential or radial membrane potential gradients in either the smooth muscle or endothelial layers of the arterioles.* This condition is required if the layers are to be modelled using conventional cable equations (16). In physiological situations this condition is almost always fulfilled, because influences which may change the membrane potential (humoral factors, innervation) are usually distributed around the vessels, assuring a uniform circumferential influence. Circumferential gradients are most likely to be a problem in

experimental situations in which a membrane potential change is induced by passing current through a microelectrode at one point in a layer; a situation that we have not modelled here. Radial gradients will be negligible in microvessels in which the muscle and endothelial layers are only one cell thick, but would have to be considered in larger vessels.

*That all cell surfaces of both layers are in contact with the extracellular fluid.* In effect, this means that the muscle and endothelium layers are separated by an extracellular space in which current can flow.

*That the electrical resistance of the extracellular space is zero.* This is a conventional assumption for this type of calculation, although its applicability in physiological situations has been questioned (25). If extracellular resistance is significant, membrane potential changes will not spread as far as they do in the examples that we give in this paper.

### **Definitions and values of cellular electrical properties**

The electrical properties of the cell layers were indicative values taken from the literature, and do not represent any particular vascular bed or species. The values and the sources on which they were based are given in Table 1.

[table 1 near here]

The intracellular resistivity for a particular layer ( $R_{ae}$  for the endothelium or  $R_{am}$  for the muscle) results from a combination of resistance due to the cytoplasm and that of intercellular junctions. Values of smooth muscle intracellular resistivity ( $R_{am}$ ) in the literature vary between 100 and 600  $\text{Scm}$ , and we have taken a value of 300  $\text{Scm}$ . For endothelial cytoplasmic resistivity we were unable to find appropriate values in the literature. We have taken the longitudinal orientation of the endothelial cells into account, and recognised that the contribution from resistance at cell-to-cell couplings will be negligible because of the greater length of uninterrupted cytoplasm between couplings, compared to the smooth muscle layer (5). It is also possible that there are more coupling structures in endothelium than in muscle (8) which will further reduce their contribution to overall resistance. Following this reasoning, we have set  $R_{ae}$  to 120  $\text{Scm}$ , the value for cytoplasm (21).

Values of the muscle to endothelium coupling resistance  $R_j$  were chosen to represent no functional coupling, moderate coupling, and very strong coupling. As there are no values for this parameter in the literature, so our values are arbitrary choices.

No coupling represents a limiting case in which  $R_j$  is very high, but it is not possible to enter infinitely high values into the NEURON program. We therefore simulated membrane potential changes in a variety of vessel networks and increased  $R_j$  from some arbitrary starting value until further increases had no effect. From this it was clear that a value of  $10^8 \text{ Scm}^2$  was large enough to represent no perceptible coupling. For the opposite extreme, very strong coupling, a value of  $R_j=0$  would be appropriate, and in this case the changes in the muscle and endothelial layers would become identical. We chose a value of  $10^2 \text{ Scm}^2$  slightly greater than 0, as this was more likely to be physically realistic and gave a just-perceptible difference between responses in the two layers (fig 5). For moderate coupling  $R_j$  was arbitrarily set to an intermediate value,  $10^4 \text{ Scm}^2$ .

## **RESULTS**

We have simulated the spread of membrane potential changes in some representative arteriolar networks which approximate common experimental situations.

In this paper we have chosen to make all conductances voltage independent, in order to illustrate the *passive* spread of membrane potential changes. The NEURON program allows

for the introduction of voltage dependent channels into the model, but the choice of appropriate channel parameters for arterioles is not clear at present. We have also chosen to set the current used to change membrane potential to a realistically small value, 0.1nA. This gives changes of the order of around 1mV, as would be required in an experiment in which it was hoped not to change voltage-dependent conductances.

[figure 2 near here]

### **No electrical coupling between layers**

A portion of an arteriolar network with the geometry shown in figure 2 was used. We have assumed that there was only one layer of muscle cells throughout the tree, and that the thickness of the muscle layer was constant throughout. Initially we assumed that the muscle and endothelium were not coupled, so as to illustrate the different electrical properties of the two layers. This was achieved by setting  $R_j$  to a very high value ( $10^8 \text{ Scm}^2$ ).

Case 1A. For this case we have assumed that the ends of the arterioles are cut and have sealed electrically, as they do in preparations of isolated arteriolar trees (11,12,7).

Figure 3 shows the membrane potential change caused by injecting a continuous 0.1nA current through a microelectrode into either the muscle or the endothelial layer. The point of current injection was positioned half way along the largest branch, as shown in figure 2.

[figure 3 near here}}

Membrane potential change was greatest at the point of current injection, falling off at either side. Towards the right the curve has multiple branches, corresponding to the membrane potential changes along the different arteriolar branches shown in figure 2.

The membrane potential change in the endothelial layer differed from that in the smooth muscle layer in two respects. The membrane potential change in the endothelium was larger at the point of current injection but decreased more rapidly with distance than that of the smooth muscle. The low internal resistivity of the endothelium facilitates the spread of membrane potential changes, whereas the small cross-sectional area of the endothelial layer hinders the spread of membrane potential changes. The overall effect with the values chosen for the model is that membrane potential changes spread further in the muscle layer than they do in the endothelium. This is shown most clearly in the lower panel of figure 3, where the voltage changes have been scaled so that their peaks are equal.

The relative spread of potential in the two layers depended on the parameter values that we chose (table 1). In order to see how sensitive our conclusions were to these choices, we varied individual parameters until spread was the same in both layers; that is, until the two curves in the lower left panel of figure 3 were superimposed. We found that endothelial thickness had to be increased to  $2\mu\text{m}$  for equal spread in the two layers, or that muscle internal bulk resistivity  $R_{\text{am}}$  had to be increased to  $1100 \text{ Scm}^2$ .

Case 1B is exactly the same as case 1A with respect to intrinsic properties of the arterioles, but represents the situation in *in vivo* preparations where the network shown in figure 2 is continuous with other vessels. The ends of the arterioles are not sealed and current can flow into the vessels to which they connect. To represent this situation for the purposes of calculation the current leaving the ends of branches has been assumed to be the same as if the branch continued indefinitely. This is a reasonable assumption which if anything slightly underestimates the current that might flow in a real network (23).

In case 1B the difference between the responses of endothelium and muscle to current injection differ in the same way qualitatively as in case 1A. Although the curve breaks up into 4 branches as in case 1A, only two are visible because after the first branching curves from the next order of branching superimpose.

### **Moderate electrical coupling between layers**

For these calculations the same network geometry and electrical parameters as case 1 have been used, except that the endothelium and muscle layers have been moderately coupled by setting  $R_j$  to  $10^4 \text{ Scm}^2$ .

As in case 1 the effect of passing a 0.1nA continuous current into one branch was simulated for both an isolated tree (case 2A) and one connected to other vessels (case 2B). Figure 4 shows the membrane potential changes in smooth muscle and endothelium expected in both types of preparation, given that the current was injected into the smooth muscle (upper pair of graphs) and, that the current was injected into the endothelium (lower pair of graphs).

[figure 4 near here]

The membrane potential change profiles of figure 4 show how moderate coupling allows a substantial amount of current to leak through from one cell layer to another. This situation resulted in smaller potential changes, and less difference between the spread of membrane potential change in the endothelium compared to that of smooth muscle. However, as in case 1, it appears that the membrane potential changes spread slightly further in the smooth muscle than in the endothelium. A current injection applied to the endothelial layer and measured in that layer (lower pair of graphs in figure 4) still results in a larger membrane potential change at the point of injection than the analogous situation for smooth muscle.

### **Strong electrical coupling between layers**

If the two layers were strongly electrically coupled, there would be no difference between the membrane potentials in the muscle and endothelial layers except in a region very close to the current source. In practice we reach this situation (case 3) when  $R_j$  has a value of approximately  $100 \text{ Scm}^2$  or less. In this case we chose the value  $100 \text{ Scm}^2$ , and figure 5 shows distribution of membrane potential changes simulated in isolated and *in vivo* networks as above.

[figure 5 near here]

### **Arteriolar tree exposed to local mediators**

For this case we consider the network shown in figure 6, which represents a small tree of arterioles connected via a feed artery (50 $\mu\text{m}$  diameter) to a larger distributing artery (90 $\mu\text{m}$  diameter). This situation might occur in a tissue such as skeletal muscle. The distributing artery was assumed to be connected to a larger network, and was made infinitely long for these calculations.

Suppose that the release of local substances from the surrounding tissue gives rise to a membrane potential change of -15 mV across the smooth muscle membrane of all small branches at the periphery of the network. The spread of membrane potential changes along the feed artery was calculated for two conditions: negligible coupling between muscle and endothelium ( $R_j = 10^8 \text{ Scm}^2$ ), and fairly strong coupling ( $R_j = 1000 \text{ Scm}^2$ ).

The calculation involved simulating a current injection into to distal end of all four arteriolar branches, and adjusting each current manually until it caused a 15mV change of membrane potential at the end of the arteriole. This involved several cycles of adjustment as each current affected the potential in all the other branches. When a change of  $-15 \pm 0.1 \text{ mV}$  at all branch ends had been obtained, the potential change along the feed artery was examined and is plotted in figure 6.

In this network the effect of changing the thickness of the muscle layer was investigated. In the initial calculations the thickness was set to 5 $\mu\text{m}$  for all vessels, as it had been for all previous calculations (fig 6A). For the result shown in figure 6B the thickness in the 50 $\mu\text{m}$  diameter "feed artery" was set to 7 $\mu\text{m}$ , and the thickness in the 90 $\mu\text{m}$  diameter vessel was set

to 9 $\mu$ m. This had virtually no effect on the rate of decay of membrane potential change along the vessel, although it did slightly decrease the overall amplitude of the change.

[figure 6 near here]

As in previous cases, the greatest membrane potential change in the smooth muscle was seen when the cell layers were not electrically coupled. There is only a marginal change in the rate of spread of membrane potential change in the muscle layer as a result of coupling to the endothelium.

It is quite likely that in a physiological situation the individual branches of an arteriolar tree would be hyperpolarised to different extents due to differences in tissue activity close to them. However, the overall result would still be some hyperpolarisation of the feed artery which would decay as we have shown.

## DISCUSSION

The examples given above illustrate several ways in which the modified version of the NEURON program can be used in modelling the behaviour of vascular networks. It extends the capabilities of previous approaches to include the possibility of electrical coupling between cells, and to explicitly include real values of cell geometry and electrical properties.

Most of our calculations have given the response to a current injection at one point in the network. The equivalent real situation would be current injection through a microelectrode, and application of a drug in one small region from a micropipette would be very similar. However, drug application differs in one important respect because of the ionic mechanism of the current generation. A drug such as ACh may generate current by opening potassium channels, and the current magnitude will depend on the difference between the membrane potential and the potassium equilibrium potential. For this reason a doubling of the dose of ACh will not necessarily cause a doubling of the current or of the resulting membrane potential change, and there will be a maximum possible hyperpolarization determined by the potassium equilibrium potential. In this paper we have used the NEURON model show the effects of specified currents rather than conductance changes. The effects of currents will add linearly provided that there are no voltage dependant conductances (which we have assumed). One example of the usefulness of our approach is illustrated in figure 3, showing that membrane potential changes do not spread as far in the endothelial layer as they do in the muscle. This result runs counter to our initial expectations which were in line with the widely held view (8) that the longitudinal orientation of the endothelial cells would ensure their dominance as a longitudinal conduction pathway. Our calculations suggest that the lower total internal resistivity is more than offset by their extreme thinness, which results in an overall high resistance in the longitudinal compared to the muscle. However, this result depends on our initial assumptions in choosing values given in table 1. Membrane resistance was the same for both layers; if we had set the resistance higher for one layer it would have increased the spread of changes in that layer. We set the internal resistivity of the endothelial to the lowest possible value, equal to that of cytoplasm alone with no contribution from coupling junctions, which would favour spread in that layer. We chose a medium value of 300  $\text{Scm}^2$  for the resistivity of the smooth muscle layer, and when we varied this value until spread in the two layers was equal we found that it required a value of 1100  $\text{Scm}^2$ , larger than any value that we have found in the literature. The other parameter that influences spread is the thickness of the layers. To increase the distance of spread in the endothelial layer we would have had to increase its thickness. Leaving the muscle layer thickness set to 5 $\mu$ m we increased

the thickness of the endothelial layer until the spread of potential changes we equal in both layers. This required an endothelial thickness of  $2\mu\text{m}$ , which is greater than many of the values in the literature, but which has been observed in constricted arterioles when the endothelium is thickened (29).

Figure 6 illustrates another point of physiological significance. When a network of arterioles in a tissue is connected to a distributing artery via a feed artery, the larger size of the distributing artery may attenuate membrane potential changes in the feed artery. In effect, membrane potential changes originating from the actions of local factors on the arterioles will not spread well in the feed arteries if the spread relies only on passive electrical properties. Coupling between the muscle and the endothelium will not significantly change the distance over which membrane potential changes spread. Given that experimental observations indicate that membrane potential changes probably do spread several millimetres along feed arteries in skeletal muscle (24), it seems likely that the spread does not rely purely on passive electrical properties, but is aided by active membrane processes.

An area in which the NEURON program may be extremely valuable is in simulating the propagation of active responses; that is the enhanced spread of membrane potential changes due the activation of voltage sensitive ion channels. Although microvessels in general do not develop strongly propagating action potentials as seen in skeletal muscle or smooth muscle of the intestine or uterus, there is clear evidence of active membrane events which assist propagation of both depolarising (23) and hyperpolarising events in arteriolar smooth muscle (4). The Neuron program already incorporates voltage sensitive channels based on Hodgkin Huxley kinetics, with provision the addition of whatever customised channels the user may wish to include. When patch clamp studies reveal the properties of voltage sensitive channels in arteriolar smooth muscle and endothelium, NEURON can assist in predicting whether they can explain records obtained from intact vessels, and thus make the link between single cell studies and microvascular physiology.

## ACKNOWLEDGEMENTS

This work was supported by grant 11613 from the National Institutes of Health, United States Public Health Service.

## REFERENCES

1. Abe Y, Tomita T. (1968) Cable properties of smooth muscle. *J Physiol* 196:87-100.
2. Bennett MR. (1972) *Autonomic neuromuscular transmission*. Cambridge University Press, Cambridge.
3. Casellas D, Bouriquet N, Moore LC. (1997) Branching patterns and autoregulatory responses of juxtamedullary afferent arterioles. *Am J Physiol* 272:F416-F421.
4. Crane GJ, Neild TO, Segal SS. (1999) The spread of hyperpolarizations in microvascular networks of the hamster cheek pouch. *Proc Aust Physiol Pharmacol Soc.* 30(2):89P.
5. Daut J, Mehrke G, Nees MS, Newman WH (1988) Passive electrical properties and electrogenic sodium transport of cultured guinea-pig coronary endothelial cells. *J Physiol* 402:237-254.
6. Delashaw JB, Duling BR. (1991) Heterogeneity in conducted arteriolar vasomotor response is agonist dependent. *Am J Physiol* 260:H1276-H1282.
7. Guibert C, Beech DJ. (1999) Positive and negative coupling of the endothelin ETA receptor to  $Ca^{2+}$ -permeable channels in rabbit cerebral cortex arterioles. *J Physiol* 514:843-56.
8. Haas TL, Duling BR. (1997) Morphology favors an endothelial cell pathway for longitudinal conduction within arterioles. *Microvascular Res* 53:113-120
9. Hines M. (1989) A program for simulation of nerve equations with branching geometries. *Int J Biomed Computing* 24:55-68.
10. Hines ML, Carnevale NT. (1997) The NEURON Simulation Environment. *Neural Computation* 9:1179-1209.
11. Hirst GDS, Neild TO. (1978) An analysis of excitatory junction potentials recorded from arterioles. *J Physiol* 280: 87-104.
12. Hirst GDS, Edwards FR, Gould DJ, Sandow SL, Hill CE. (1997) Electrical properties of iridial arterioles of the rat. *Am J Physiol* 273:H2465-H2472.
13. Hua C, Cragg B. (1980) Measurements of smooth muscle cells in arterioles of guinea-pig ileum. *Acta Anat* 107:224-230.
14. Jack JJB, Redman SJ. (1971) The propagation of transient potentials in some linear cable structures. *J Physiol* 215:283-320.
15. Lash JM. (1996) Regulation of skeletal muscle blood flow during contractions. *Soc for Expt Biol & Med* 211:218-235.
16. Neild TO. (1983) The relation between the structure and innervation of small arteries and arterioles and the smooth muscle membrane potential changes expected at different levels of sympathetic nerve activity. *Proc. R. Soc. Lond. B* 220:237-249.
17. Pacicca C, Schaad O, Beny J-L. (1996) Electrotonic propagation of kinin-induced, endothelium-dependent hyperpolarizations in pig coronary smooth muscles. *J Vasc Res* 33:380-385.
18. Rall W. (1964) Theoretical significance of dendritic trees for input-output relations. In: *Neural Theory and Modeling*. (R.F. Reiss, Ed.) Stanford University Press, Stanford, CA. 73-94.
19. Rhodin JAG (1967) The ultrastructure of mammalian arterioles and precapillary sphincters. *J Ultrastruct Res* 18:181-223.
20. Rhodin JAG (1980) Architecture of the vessel wall. In: *Handbook of Physiology* Section 2 Vol II (DF Bohr, AP Somlyo, HV Sparks, Eds) American Physiological Society, Bethesda Maryland. 1-32.
21. Schanne OF. (1969). Measurement of cytoplasmic resistivity by means of the glass

- microelectrode. In *Glass Microelectrodes*. (Lavalley M, Schanne OF, Hebert NC, Eds.) John Wiley, New York. 299-321.
22. Segal SS. (1994) Cell-to-cell communication coordinates blood flow control. *Hypertension* 23:1113-1120.
  23. Segal SS, Neild TO. (1996) Conducted depolarization in arteriole networks of the guinea-pig small intestine: effect of branching on signal dissipation. *J Physiol* 496:229-244.
  24. Segal SS, Welsh DG, Kurjiaka DT. (1999) Spread of vasodilatation and vasoconstriction along feed arteries and arterioles of hamster skeletal muscle. *J Physiol* 516:283-291.
  25. Sperelakis N, Marschall RA, Mann JE. (1983) Propagation down a chain of excitable cells by electric field interactions in junctional clefts: effect of variation in extracellular resistances, including a "sucrose gap" simulation. *IEEE Transactions in Biomedical Engineering* 30:658-664.
  26. Steinhausen M, Endlich K, Nobiling R, Parekh N, Schutt F. (1997) Electrically induced vasomotor responses and their propagation in rat renal vessels in vivo. *J Physiol* 505:493-501.
  27. Vargas FF, Caviedes PF, Grant DS. (1994) Electrophysiological characteristics of cultured human umbilical vein endothelial cells. *Microvasc Res* 47:153-165.
  28. Wagner AJ, Holstein-Rathlou -H, Marsh DJ. (1997) Internephron coupling by conducted vasomotor responses in normotensive and spontaneously hypertensive rats. *Am J Physiol* 272: F372-F379.
  29. Walmsley J, Gore R, Dacey, RG Jr, Damon D, Duling B. (1982) Quantitative morphology of arterioles from the hamster cheek pouch related to mechanical analysis. *Microvasc Res* 24:249-271.
  30. Welsh DG, Segal SS. (1998) Endothelial and smooth muscle conduction in arterioles controlling blood flow. *Am J Physiol* 274:H178-H186.
  31. Xia J, Duling BR. (1995) Electromechanical coupling and the conducted vasomotor response. *Am J Physiol* 269:H2022-H2030.

Parameter	symbol	value	source
Thickness of the muscle layer	$\delta$	5 $\mu\text{m}$	8,13,19
Muscle specific membrane resistance	$R_{\text{mm}}$	$5 \times 10^4 \text{ Scm}^2$	11
Muscle intracellular resistivity	$R_{\text{am}}$	300 $\text{Scm}$	2,11,12
Thickness of the endothelial layer	$\delta$	0.5 $\mu\text{m}$	8,12
Endothelium specific membrane resistance	$R_{\text{me}}$	$5 \times 10^4 \text{ Scm}^2$	5,27
Endothelium intracellular resistivity	$R_{\text{ae}}$	120 $\text{Scm}$	see text
Muscle to endothelium coupling resistance	$R_j$	(Varied) $\text{Scm}^2$	

Table 1 The membrane electrical properties used in the calculations. The values were based on information in the references, and are representative of mammalian arteriolar tissue rather than specific to any particular vascular bed or species.

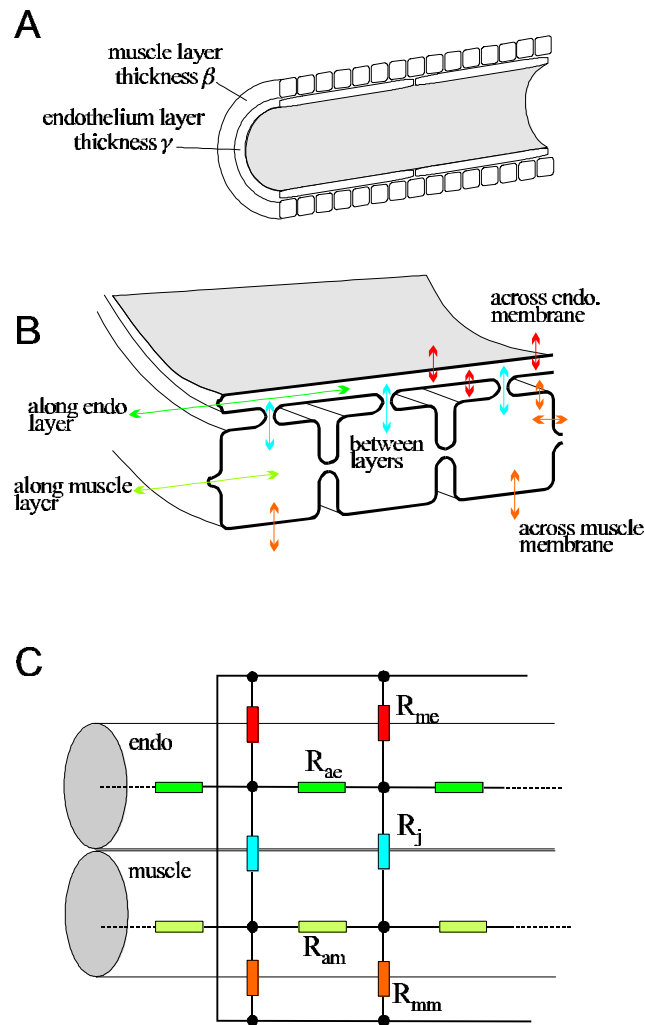


Figure 1 (A) Diagram showing a microvessel consisting of a layer of endothelial cells of thickness  $\gamma$ , surrounded by a layer of smooth muscle cells of thickness  $\beta$ . (B) An enlarged section of A, showing the possible electrical conduction pathways between the individual cells and across the cell membranes to the extracellular space. The actual current pathway in any particular situation will depend on the point at which current is injected. (C) The equivalent electrical circuit for the model illustrated in B.

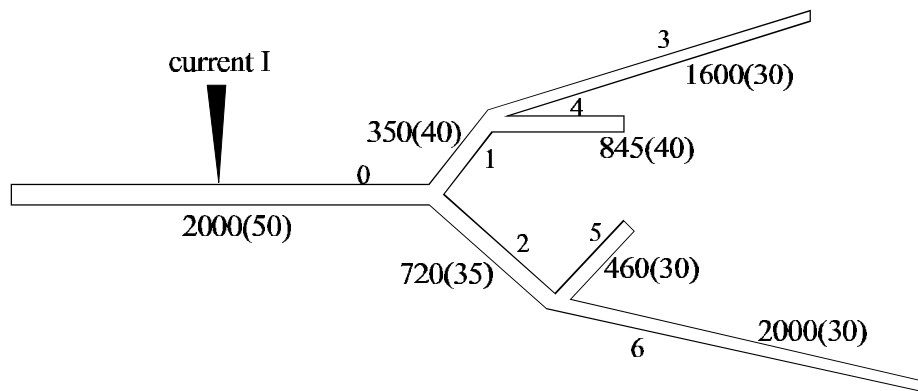


Figure 2. Schematic of the arteriole network used for the calculations. Branches are numbered from 0 to 6. The length and diameter (in brackets) in microns of each branch is shown.

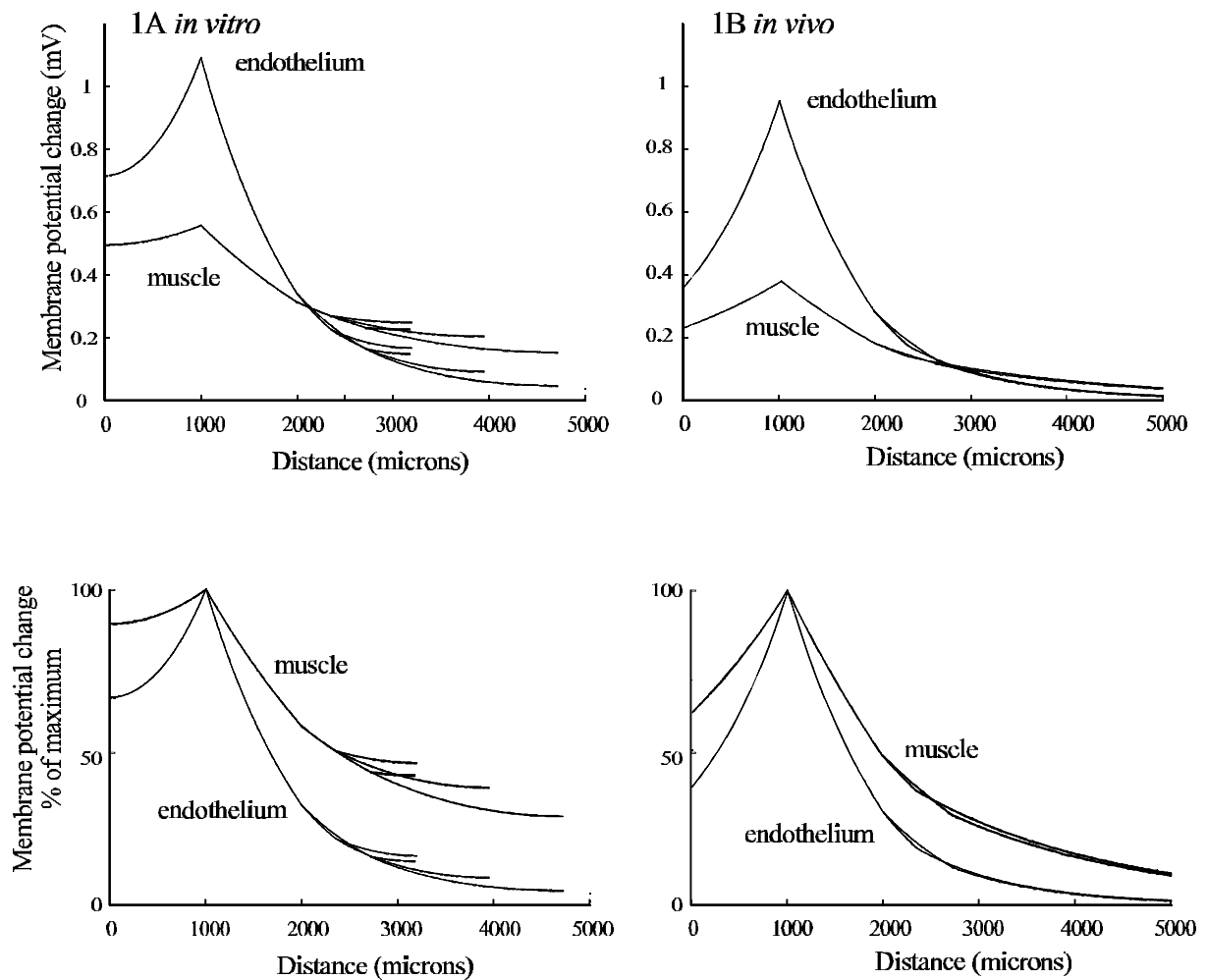
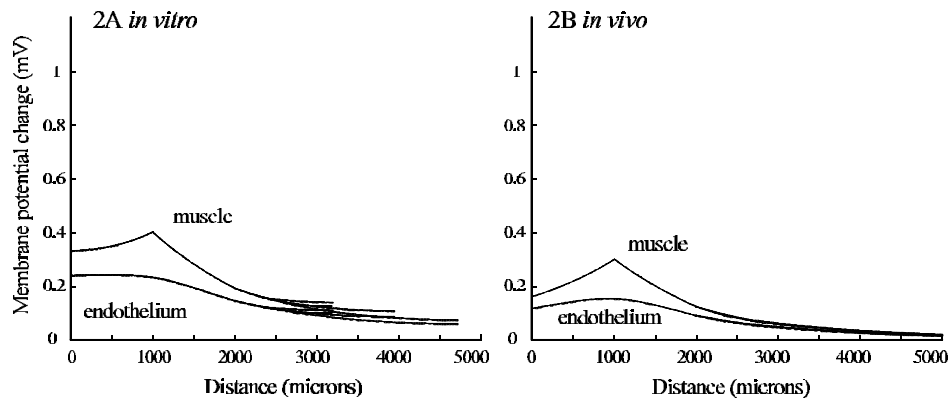


Figure 3. No coupling between smooth muscle and endothelium. Membrane potential changes along the endothelium and smooth muscle resulting from the injection of a continuous 0.1nA current at the midpoint of the largest branch in the network shown in figure 2. 1A shows the distribution of membrane potential change in an *in vitro* preparation with electrically sealed ends, whereas, 1B shows that an *in vivo* preparation in which current spreads to other vessels. Upper panels show the membrane potential change in mV, lower panels show the same records normalised to the peak membrane potential change in order to show the relative extent of spread in the two layers.

### Current injection into muscle layer



### Current injection into endothelial layer

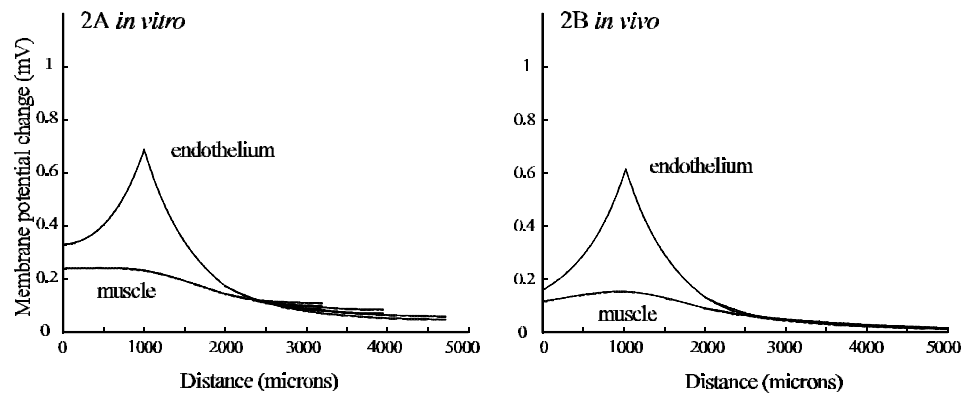


Figure 4. Moderate coupling between smooth muscle and endothelium. Membrane potential changes along the endothelium and smooth muscle resulting from injection of a continuous 0.1nA current into one of the layers, as shown in figure 2. Upper: current injection into muscle layer. Lower: current injection into endothelium. In both pairs of graphs, 2A shows the distribution of membrane potential change in an *in vitro* preparation, whereas 2B shows that of an *in vivo* preparation. At distances beyond 2000 $\mu$ m the curves have multiple branches, corresponding to the membrane potential changes along the different arteriolar branches.

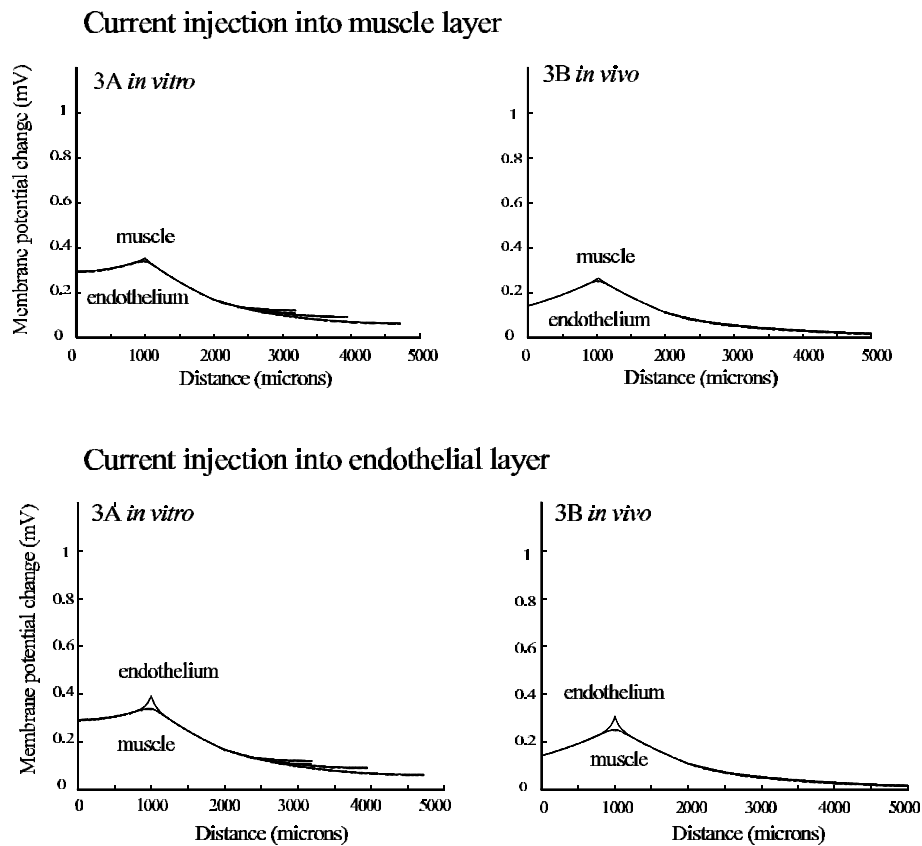


Figure 5. Strong coupling between smooth muscle and endothelium. Membrane potential changes along the endothelium and smooth muscle resulting from injection of a continuous 0.1nA current into one of the layers, as shown in figure 2. Upper: current injection into muscle layer. Lower: current injection into endothelium. In both pairs of graphs, 2A shows the distribution of membrane potential change in an *in vitro* preparation, whereas 2B shows that of an *in vivo* preparation.

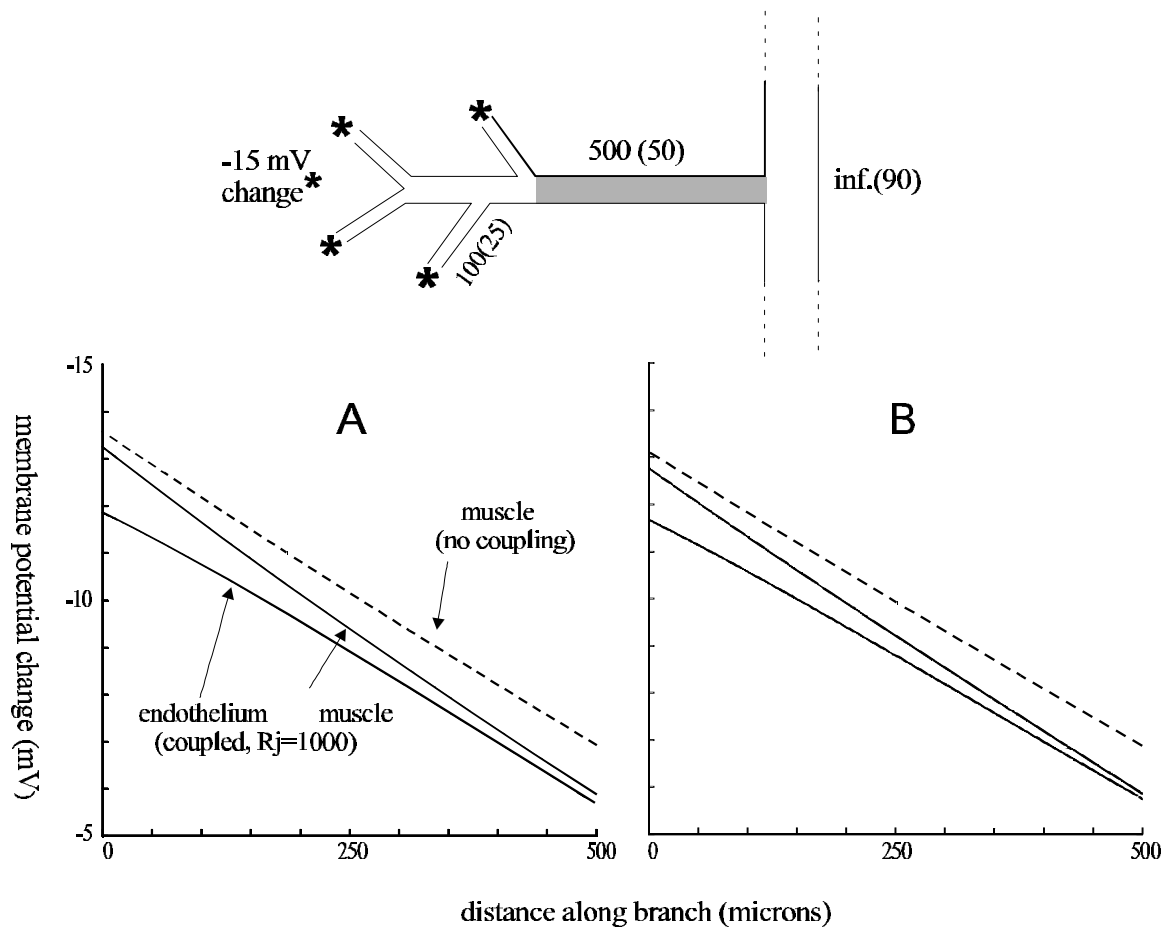


Figure 6. An arteriolar network designed to simulate the situation of an arteriolar tree connected to a feed artery, in which only the arterioles are subject to metabolic factors from the tissue which change membrane potential. A -15 mV change was imposed on the smooth muscle layer at the end of each of the peripheral branches.

A, B. Membrane potential changes on the shaded branch in response to a -15 mV change on the periphery of the network. Membrane potential spread along the shaded branch is shown for smooth muscle (central curve) and endothelium (lower curve) when the two cell layers are quite strongly coupled ( $R_j=1000\text{Scm}^2$ ). The upper curve shows the distribution of membrane potential in the smooth muscle layer when there is no electrical coupling to the endothelium. A. Thickness of the muscle layer  $5\mu\text{m}$  in all regions. B. Thickness of the muscle layer increased for the larger branches:  $7\mu\text{m}$  in the shaded branch for which potential changes are shown,  $9\mu\text{m}$  for the larger arteriole to its right,  $5\mu\text{m}$  for all other segments.